

Methodology for the structural analysis of a main deck of FPSO vessel supporting an offshore crane

Metodología para el análisis estructural de una cubierta principal de un buque FPSO soportando una grúa sobre orugas

Diego Hernández-Méñez ¹, Iván Félix-González ², José Hernández-Hernández ³, Agustín L. Herrera-May ⁴

¹ Faculty of Construction and Habitat Engineering, Universidad Veracruzana, México. Email: hemdf387@gmail.com

² Center for Exploration and Production Technologies, Mexican Petroleum Institute, Mexico.

Orcid: [0000-0001-9837-6433](https://orcid.org/0000-0001-9837-6433). Email: ifelix@imp.mx

³ Faculty of Mechanical Engineering and Naval Sciences, Universidad Veracruzana, México.

Orcid: [0000-0003-1781-9074](https://orcid.org/0000-0003-1781-9074). Email: josehernandez02@uv.mx

⁴ Micro and Nanotechnology Research Center, Universidad Veracruzana, México.

Orcid: [0000-0002-7373-9258](https://orcid.org/0000-0002-7373-9258). Email: leherrera@uv.mx

Received: 15 March 2022. Accepted: 26 August 2022. Final version: 3 November 2022.

Abstract

Offshore cranes placed on the surface of Floating Production Storage and Offloading (FPSO) vessels affect the structural response of their main decks, which can alter the safe operation of the FPSO vessels. Generally, classification societies rules are used to predict the structural strength of the main deck of FPSO vessels. However, these classification societies rules are limited to estimate the variation of the structural performance of the main deck caused by the operation of offshore cranes under different hydrodynamic conditions. Here, we present a methodology to determine the alteration of the structural behavior of a main deck of FPSO vessel due to different operation conditions of a board offshore crane. This methodology considers the hydrodynamic response for two ultimate limit states: operating and storm conditions from 1000 m water depth in Gulf of Mexico with a return period of 10 and 100 years, respectively. The methodology includes finite element method (FEM) models of the main deck supporting an offshore crane to predict its structural response. The maximum von Mises stress of the main deck does not overcome its maximum permissible stress, which allows a safe operation of the FPSO crane. The proposed methodology can be used to estimate the structural behavior of main decks of FPSO vessels that are modified for supporting offshore cranes, regarding the hydrodynamic response for each FPSO under the operation and extreme conditions in its location. Thus, naval designers could select the better structural modifications of the main decks that decrease their costs of construction and maintenance.

Keywords: Main deck; FEM; FPSO; structural analysis; offshore crane; vessels.

Resumen

Las grúas montadas mar adentro sobre las superficies de buques de producción, almacenamiento y abastecimiento (FPSO, por sus siglas en inglés) afectan la respuesta estructural de sus cubiertas principales, las cuales pueden alterar

ISSN Printed: 1657 - 4583, ISSN Online: 2145 - 8456.

This work is licensed under a Creative Commons Attribution-NoDerivatives 4.0 License. [CC BY-ND 4.0](https://creativecommons.org/licenses/by-nd/4.0/)



How to cite: D. Hernández-Méñez, I. Félix-González, J. Hernández-Hernández, A. L. Herrera-May, "Methodology for the structural analysis of a main deck of FPSO vessel supporting an offshore crane," *Rev. UIS Ing.*, vol. 22, no. 1, pp. 1-16, 2023, doi: <https://doi.org/10.18273/revuin.v22n1-2023001>

la operación segura de los buques FPSO. Generalmente, las reglas de sociedades de clasificación son usadas para predecir la resistencia estructural de la cubierta principal de buques FPSO. Sin embargo, estas reglas están limitadas para estimar la variación del comportamiento estructural de la cubierta principal causada por la operación de engranes mar adentro con diferentes condiciones hidrodinámicas. Este artículo presenta una metodología para determinar la alteración del comportamiento estructural de una cubierta principal de un buque FPSO debido a diferentes condiciones de operación de una grúa sobre orugas. Esta metodología considera la respuesta hidrodinámica para dos estados límites últimos: condiciones de operación y tormenta desde una profundidad de mar de 1000 m en Golfo de México con periodos de retorno de 10 y 100 años, respectivamente. La metodología incluye modelos del método de elementos finitos de la cubierta principal soportando una grúa sobre orugas para predecir su respuesta estructural. El máximo esfuerzo de von Mises de la cubierta principal no supera el máximo esfuerzo admisible, lo cual permite un funcionamiento seguro del engrane mar adentro. La metodología propuesta puede ser usada para estimar el funcionamiento estructural de cubiertas principales de buques FPSO que son modificadas para soportar grúas mar adentro, considerando las respuestas hidrodinámicas para cada buque sujetas a condiciones de operación y extremas en su localización. Así, diseñadores navales podrían seleccionar las mejores modificaciones estructurales de las cubiertas principales que disminuyan sus costos de construcción y mantenimiento.

Palabras clave: cubierta principal; FEM; FPSO; análisis estructural; grúa mar adentro; buques.

1. Introduction

Floating Production Storage and Offloading (FPSO) vessels operate in remote ocean areas transporting materials and equipment, which are operated by offshore cranes. Commonly, the offshore cranes are not examined in the initial design stage of FPSO vessels [1], [2]. The installation or replacement of offshore cranes in FPSO vessels requires the structural analysis of their main decks to predict the variation of the structural behavior due to the operation of the offshore cranes. In addition, the performance of offshore cranes can be affected by the environmental and hydrodynamic conditions [3].

The American Petroleum Institute (API) recommends structural calculations to study the static design of an offshore crane considering a safety factor of 2, which is related to the static load and allowable tension of the crane [4]. The structural analysis of FPSO vessels supporting offshore cranes can contemplate both cases the crane at rest under storm and the crane in operating condition. Ozguc [5] proposed non-linear finite elements method (FEM) models using the LS-DYNA software to obtain the structural evaluation of a deck of FPSO vessel due to dopped objects from cranes. These models can determine the impact damage on the deck generated by various dropped object types.

However, this Ozguc investigation did not include the structural analysis of the connection area between the deck and the crane. Lee et al. [6] investigated the effect of the operation modes of gantry cranes of FPSO vessel on the wind forces that act on the vessel. For this, they registered different wind tunnel tests on the FPSO vessel model, which was scaled of 1:200. The operating condition of the cranes increased the wind forces by up 8.6% in comparison with the parking mode of the cranes.

Shin [7] reported the fatigue analysis for offshore cranes using a load-spectrum model, which regarded three years of data registered for three offshore cranes. Thus, Shin presented an adequate loadspectrum model to acquire a detailed fatigue analysis of the offshore cranes. Khudhur [8] developed FEM models through ANSYS software to predict the maximum deflections and stress distribution of a crane boom. Nevertheless, these models did not consider the operating conditions of the crane.

The crane pedestal is a critical structural element of the crane due to that supports the loads and flexural moments during the crane operation. Krukowski et al. [9] designed FEM models of the pedestal, the frame, and the boom of an offshore column crane to estimate the dynamic structural behavior of these components. The structural analysis of different marine structures can be studied using FEM models [10]. These models can regard the wave load effects on the structural strength of the ships [11]. Furthermore, classification societies can be employed to assessment the structural safety of marine structures considering high dynamic factors [12], [13].

Although, these high dynamic factors can alter the real effect of the loads on the structural behavior of the marine structures. Here, we propone a methodology to determine the structural response of a main deck of FPSO vessel supporting a BOS 2600 offshore crane [14]. This methodology incorporates the hydrodynamic loads on the FPSO vessel located to 1000 m water depth in the Gulf of Mexico with environmental data from two ultimate limit states.

These states evaluate the operational crane conditions with a return period of 10 years and extreme conditions with a return period of 100 years, corresponding to

hurricane, when the crane boom rests on its support. This methodology comprises the dynamic response of the critical operating points of the offshore crane without the standard dynamic factor used in the classification societies rules. Our methodology uses FEM models to estimate the von Mises stress distribution on the crane pedestal and the FPSO main deck. This methodology gives us a more rational design of crane pedestal and reinforcement of main deck, in where the pedestal is connected. Thus, the pedestal design and reinforcement of the main decks can be optimized to select the best installation positions of the offshore cranes on the main decks that ensure their safe performance.

This work is structured as follows: Section 2 describes the methodology to predict the structural performance of a main deck of FPSO vessel that supports an offshore crane under different operating and environmental conditions. This methodology comprises the development of 3D hull models, hydrodynamic analysis, determination of forces and moments components on the crane pedestal, and the structural analysis of the main deck. Section 3 shows the results and discussion of the structural response of the main deck. Finally, we depict the conclusions and advantages of the proposed methodology.

2. Theoretical description

Our methodology (Fig. 1) for the structural analysis of a main deck of FPSO vessel supporting an offshore crane has the following four stages:

(i) Stage 1: A 3D hull model of FPSO vessel is developed using Sesam GeniE software. This model contains the compartments of the hull. This hull is modeled by defining compartments, wet area, and loads for each storage tank. This complements the required information by the HydroD SeSam DNV module. Thus, time and costs are decreased to evaluate new hull designs, out-of-design equipment installed on the deck or repair offshore cranes areas.

(ii) Stage 2: The hydrodynamic analysis of the 3D hull model is obtained with HydroD Sesam DNV software, including the data processing with PostResp Sesam DNV. This data processing is delimited to the operational area of the FPSO. For this case, the data regard the operational environmental contours in Gulf of Mexico with a return period of 10 years to assess the FPSO hydrodynamic response for crane operation conditions at the location. Moreover, the data register the extreme storm environmental contours in Gulf of

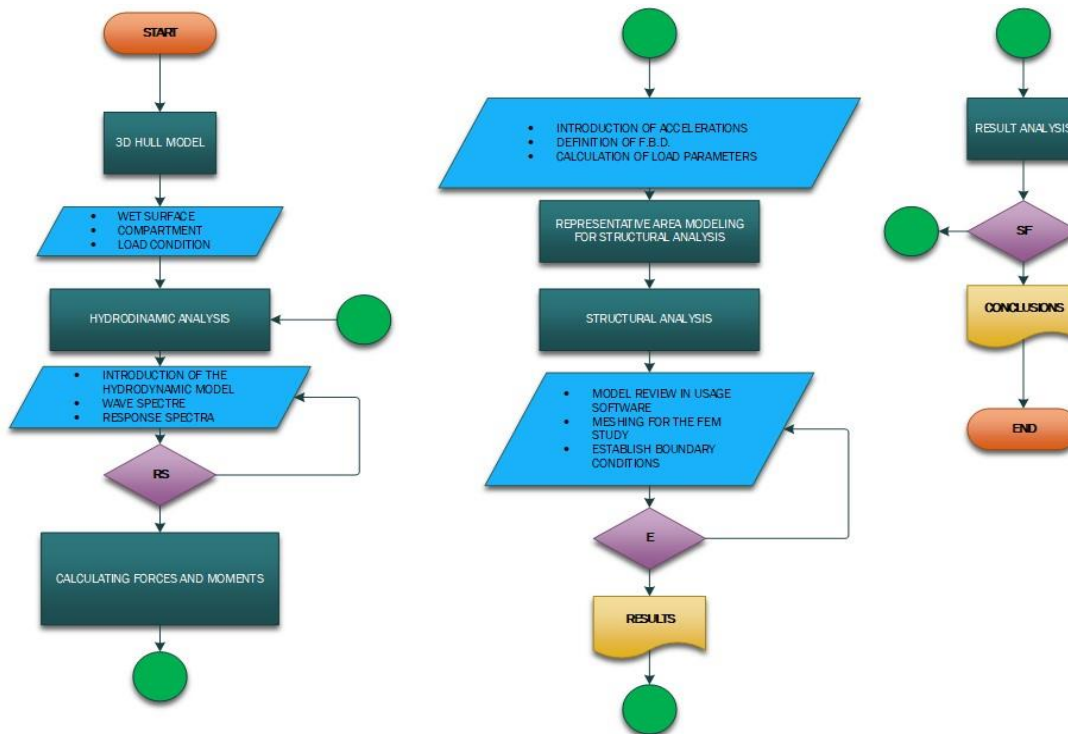


Figure 1. Flowchart of the stages of the methodology proposed for the structural analysis of a main deck of the FPSO vessel supporting an offshore crane.

Mexico considering a return period of 100 years to assess the FPSO hydrodynamic response when the crane boom is resting on its support. With these data, the maximum accelerations and forces at critical points of the crane support are determined considering the maximum load in operating conditions and in boom rest position for extreme storm at FPSO location.

(iii) Stage 3: The accelerations of the FPSO are estimated using the hydrodynamic response. Later, forces and moments on the pedestal of the offshore crane are calculated employing operational and extreme storm conditions.

(iv) Stage 4: The structural analysis of a FEM model of the FPSO main deck is reported using ANSYS

software. This FEM model adds the pedestal of the offshore crane.

2.1. Hull model of the FPSO

The 3D hull model (Fig. 2) of the FPSO vessel is drawing using Sesam GeniE software. This model incorporates the different compartments for the crude oil and ballast water storage tanks, and equipment modules of the FPSO (Figs. 3 and 4). The equipment modules represent additional weight on the FPSO. Figure 5 shows the 3D model that include the wet area of the FPSO vessel, which is obtained through Sesam GeniE software. Figure 6 depicts the mesh of the 3D model of the FPSO vessel, which include the masses related with equipment modules.

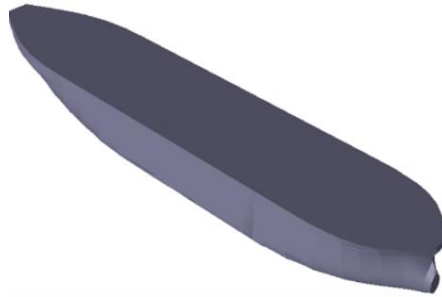


Figure 2. 3D hull model of the FPSO vessel, which is developed using Sesam GeniE software.

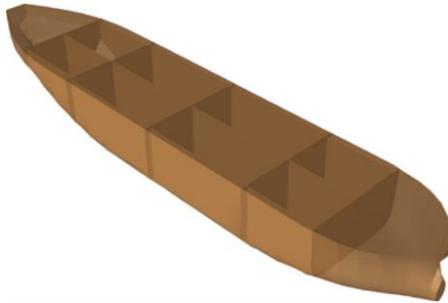


Figure 3. 3D hull model including different compartments of the FPSO vessel, which is generated with Sesam GeniE software.

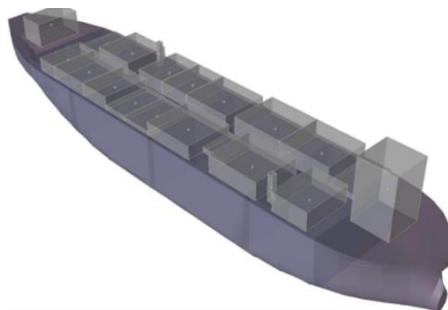


Figure 4. 3D hull model considering equipment modules of the FPSO vessel, which is obtained with Sesam GeniE software.



Figure 5. 3D hull model incorporating the wet surface of the FPSO vessel, which is elaborated through Sesam GeniE software.

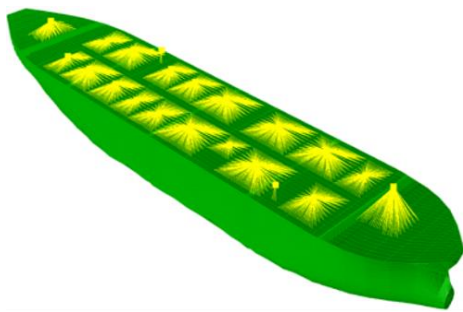


Figure 6. Mesh of the 3D hull model of the FPSO vessel, adding the masses of the equipment modules. This model is developed using Sesam GeniE software.

2.2. Hydrodynamic Analysis

The hydrodynamic analysis of the 3D hull model of the FPSO vessel examines the following points:

- (i) Hydrodynamic analysis with and without viscous damping. This point is used to demonstrate the difference between the results of the vessel behavior when its Response Amplitude Operator (RAO) is determined.
- (ii) Nine orientations of the action of the oceanic environment are established to describe the position of the vessel with respect to the plane. This position has a range from 120 to 240 degrees with increments of 15°.
- (iii) Three drafts (10 m, 15 m, and 20 m) are studied to obtain the critical operation condition, considering the highest load on the vessel.

These points are the initial conditions for the hydrodynamic analysis of the FPSO vessel. The wave periods are established in where the energy generated by the waves is significant and the maximum value of the period is set to 30 seconds. The period starts at 3 seconds because the energy of the wave begins to be relevant in

that period. The properties of the environmental fluids and gravity value used in the hydrodynamic analysis of the FPSO vessel are the follows: gravity of 9.80665 m/s², water depth of 1000m, air density of 1.226 kg/m³, air kinematic viscosity of 1.462 x 10⁻⁵ m²/s, water density of 1025 kg/m³, and water kinematic viscosity of 1.19 x 10⁻⁶ m²/s. The characteristics of the working fluids inside the FPSO tanks are established. For each load condition, the filling level of each tank is calculated to use the ideal equilibrium condition for each draft. Therefore, the density of each fluid is required (Table 1). Fluids that interact inside the vessel are defined.

The equilibrium condition of the FPSO for each load condition depends on the filling level of the tanks. The tanks are individually configured to calculate the equilibrium condition. Figure 7 illustrates the 3D model with the equilibrium condition of the FPSO vessel, which is obtained using Sesam HydroD software. Next, the hydrodynamic analysis of the FPSO vessel determines the offbody points, which define the representative space of the sea level (Fig. 8). Two cases for the hydrodynamic analysis were generated to include the viscous damping of the vessel.

Table 1. Densities of the cargo fluids inside the FPSO tanks

Cargo fluids	
Crude oil	900 kg/m ³
Seawater (ballast)	1025 kg/m ³

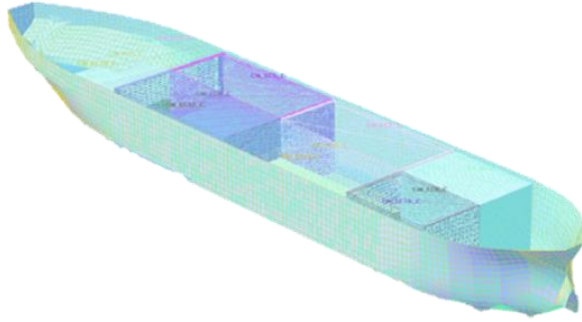


Figure 7. 3D hull model with equilibrium condition of the FPSO vessel, which is obtained using Sesam HydroD software.

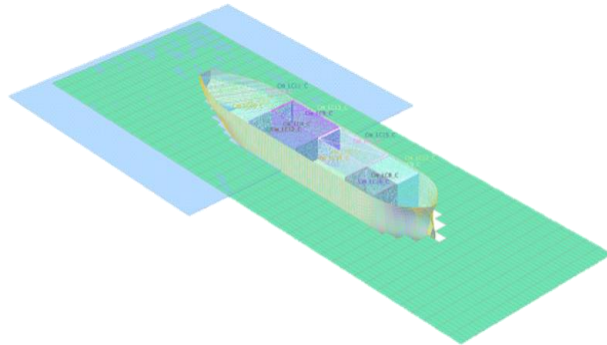


Figure 8. 3D hull model of the FPSO vessel considering the sea level for its hydrodynamic analysis through Sesam HydroD software.

2.3. Crane Installation Effects

In the operating points of the BOS 2600 offshore crane, the accelerations were calculated for both regular working conditions (calm sea) and hurricane conditions, as shown in Figs. 9 and 10. In these points, the maximum load of the crane is considered. The origin point of the coordinate system is located on the aft of the FPSO vessel (Figs. 9 and 10). Figure 9 shows the different angles used to calculate the operating points of the offshore crane, including both bow and aft sections on the FPSO vessel.

During storm conditions, the offshore crane must have a rest position. To determine the coordinates of the operating points of the crane, the coordinates of the crane cabin base (X_c, Y_c, Z_c) are included in Table 3. Thus, these operating points (Table 2) can be defined by the following equations:

$$X_p = X_c + R \cos\left(\frac{\pi D_{op}}{180}\right) \quad (1)$$

$$Y_p = Y_c + R \sin\left(\frac{\pi D_{op}}{180}\right) \quad (2)$$

$$Z_p = Z_c + Z_T \quad (3)$$

where R is the radius at maximum load capacity, D_{op} is the operation direction in degrees, and Z_T is the total boom height position. For our offshore crane, $R = 15$ m.

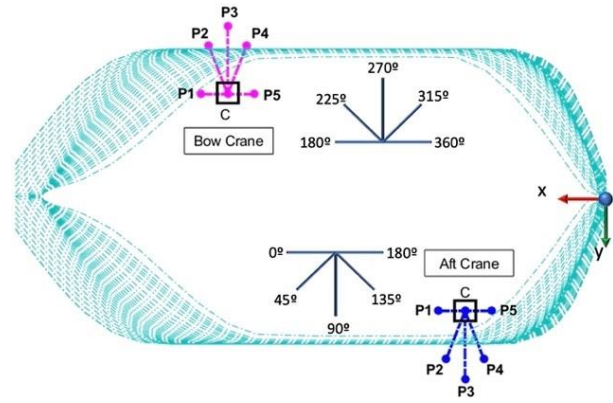


Figure 9. Five operating points of the offshore crane on both bow and aft sections of the FPSO vessel under operating conditions (calm sea).

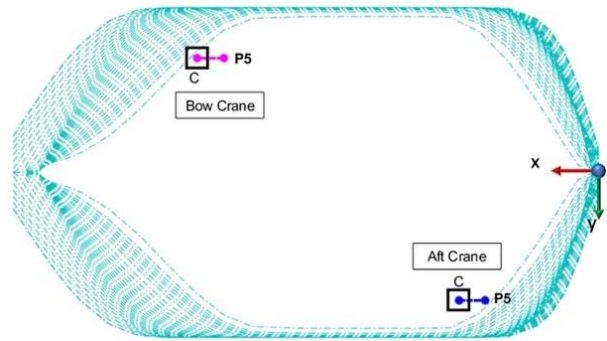


Figure 10. Operating points of the offshore crane on both bow and aft sections of the FPSO vessel under hurricane conditions.

The RAOs describe the behavior of the vessel for the six degrees of freedom per unit wave amplitude. Wave spectra are considered (S_w) based on the contours of waves with a return period of 100 years, which describe the environmental conditions at the specific location (hypothetically). Next, the model response spectra (S_R) are obtained. These spectra describe the motions of the vessel under the environmental conditions. The (S_R) is calculated with the following equation:

$$S_R = S_w + (RAOs)^2 \quad (4)$$

These spectra include low sea ridges, allowing each wave to be selected with a specific weight. It is generated through a wave propagation function, usually a cosine

function. Each response spectrum has assigned a control number, which will be the reference for the analysis of the results.

2.4. Calculation of Applied Forces and Moments

Data from the previous block describe the maximum accelerations at the critical operating points of offshore crane [15]. These data are used to calculate the force and moment components on the crane pedestal and main deck.

First, three points of the crane are defined to determine the loads: cab and tip of the boom at the points considered in the previous block.

Table 2. Coordinates of the offshore crane operating points for both bow and aft sections of the FPSO vessel

Crane	Point	Dop	X	Y	Z
Bow	C		248.250 m	-25.182 m	46 m
	P1	180°	233.250 m	-25.182 m	101 m
	P2	225°	237.643 m	-35.789 m	101 m
	P3	270°	248.250 m	-40.182 m	101 m
	P4	315°	258.857 m	-35.789 m	101 m
	P5	360°	263.250 m	-25.182 m	101 m
Aft	C		113.750 m	22.500 m	46 m
	P1	0°	128.750 m	22.500 m	101 m
	P2	45°	124.357 m	33.107 m	101 m
	P3	90°	113.750 m	37.500 m	101 m
	P4	135°	103.143 m	33.107 m	101 m
	P5	180°	98.750 m	22.500 m	101 m

Table 3. Maximum values of the force and moment components that are calculated from acceleration components at the analysis points on the offshore crane pedestal

Regular operating conditions (calm sea)							
Crane	Point	Force components (N)			Moment components (Nm)		
		F_x	F_y	F_z	M_x	M_y	M_z
Bow	P1	38.63	219.73	-734.62	12324.33	-13185.93	3295.95
	P2	40.22	219.97	-748.64	20278.33	-10196.31	1906.56
	P3	40.89	220.57	-756.10	23712.89	-2293.38	-613.35
	P4	40.22	221.17	-751.99	20381.04	5720.32	-2772.44
	P5	38.63	221.47	-740.31	12421.77	8937.93	3322.05
Aft	P1	39.51	105.91	-707.37	5939.33	-12826.79	1588.56
	P2	41.01	103.45	-712.47	13358.49	-9856.86	662.25
	P3	41.64	102.79	-716.34	16517.76	-2335.55	-624.65
	P4	41.01	102.13	-716.34	13325.56	5297.98	-1518.14
	P5	39.51	104.05	-713.18	5835.17	8481.46	-1560.68

*This case considers the crane on the bow and aft sections of the FPSO vessel for regular operating conditions.

Figure 11 depicts the schematic view of the three points selected to predict the force and moment components. These force components are given by

$$F = ma \quad (5)$$

where m represents the masses of the cab and load, respectively, and a is the acceleration at location point. For the BOS 2600 offshore crane, we use 10 ton and 60 ton for the cab and load masses, respectively. For our case, we employ 60 ton as maximum load for the crane to avoid the rolling and stability problems of the vessel. Figure 12 illustrates the free body diagram of the crane that describes the forces at each work point, including the pedestal. The total force (F_T) for each cartesian component is established as the sum of the acting forces at the top of the boom (F_b) and the cab (F_c), respectively.

$$F_T = F_c + F_b \quad (6)$$

After that these forces are calculated, the moments corresponding to them are also determined. First, the distances from the origin of each cartesian axis to the force components are defined. They must be established between the base of the crane pedestal and the point of interest (cab and boom). These distances are obtained as follows:

$$X'' = x_c - X_p \quad (7)$$

$$Y'' = y_c - Y_p \quad (8)$$

$$Z'' = z_c - Z_p \quad (9)$$

$$X' = x_b - X_p \quad (10)$$

$$Y' = y_b - Y_p \quad (11)$$

$$Z' = z_b - Z_p \quad (12)$$

where X' , Y' , and Z' are the distances measured from top of the crane boom and X'' , Y'' , and Z'' are the distances acquired from crane cab. These distances and forces are required to calculate the moment components (see Fig. 13) on the crane cockpit (M_c) and the crane base (M_{BG}), respectively.

$$M_c = \det \begin{bmatrix} i & j & k \\ F_{xc} & F_{yc} & F_{zc} \\ X'' & Y'' & Z'' \end{bmatrix} \quad (13)$$

$$M_{BG} = \det \begin{bmatrix} i & j & k \\ F_{xb} & F_{yb} & F_{zb} \\ X' & Y' & Z' \end{bmatrix} \quad (14)$$

Finally, the total moment on the crane pedestal is established as:

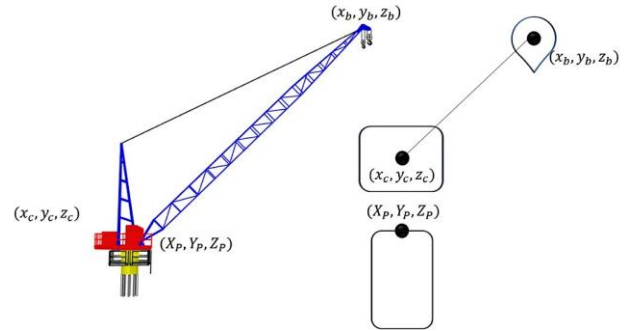


Figure 11. Schematic view of the three points of the offshore crane used to calculate the force and moment components.

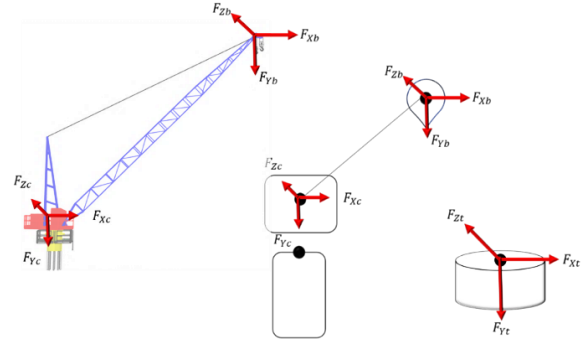


Figure 12. Free body diagram of the offshore crane that includes the force components on the work points of the crane, considering the crane pedestal.

$$M_T = M_c + M_{BG} \quad (15)$$

The values of the force and moment components applied to the crane pedestal are the load conditions used in the structural analysis. These components are obtained with the highest acceleration of hydrodynamic analysis results.

Table 3 and 4 indicate the maximum values of forces and moment components calculated from acceleration components, at handling points of the offshore crane pedestal considering the crane in bow and aft sections, and regular operating (calm sea) and hurricane (storm) conditions, respectively.

Table 4. Maximum values of force and moment components that are obtained from the acceleration components at the analysis points on the offshore crane pedestal

Hurricane conditions (storm)							
Crane	Point	Force (N)			Moment (Nm)		
		Fx	Fy	Fz	Mx	My	Mz
Bow	C	57.89	405.41	-767.07	16.36	-5.21	0
	P5	57.89	405.41	-767.07	22,738.65	8259.03	-6081.15
Aft	C	58.99	193.3	-737.42	16.36	-5.21	0
	P5	58.99	193.3	-737.42	16.36	7752.88	-6081.15

*This case assesses the crane at rest on the bow and aft sections of the FPSO vessel for hurricane conditions (storm).

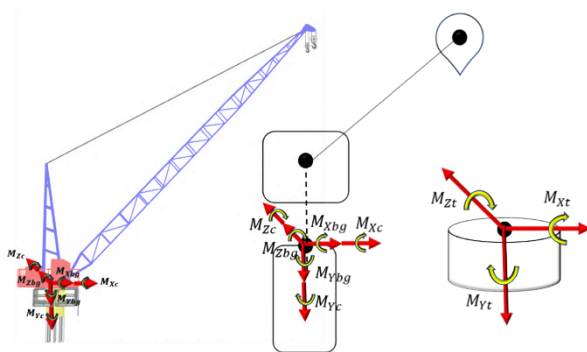


Figure 13. Free body diagram of the moment components on the offshore crane pedestal.

2.5. 3D model of the Crane Pedestal Support Frame

Figure 14 depicts a 3D model of the crane pedestal support frame that transversally considers the distance from the overboard to the crunch of the FPSO vessel (center). In addition, this FEM model adds a first arrangement of structural reinforcements and a plate thickness of 15 mm for the structural steel of the main deck.

For the structural analysis of the crane pedestal support frame, two geometries (A and B) were considered. The geometry A (Fig. 15 a) includes the representation of a part of the main deck with the crane pedestal to the waterline. The geometry B (Fig. 15 b) reports the full 3D model of the crane pedestal support frame.

2.6. 3D model of the Crane Pedestal Support Frame

The previous steps described the process to obtain the data for the operating zone of the main deck of the FPSO vessel supporting an offshore crane. In this sub-section, the structural analysis of the crane pedestal support

frame of the main deck of the FPSO vessel is presented. For this, a 3D model of the crane pedestal support frame is drawn using Inventor software, as shown in Figure 16. This 3D model contains components with more structural details to be used in the FEM simulations with ANSYS software. Table 5 shows the properties of the structural steel employed for the FEM simulations of the 3D model of the crane pedestal support frame.

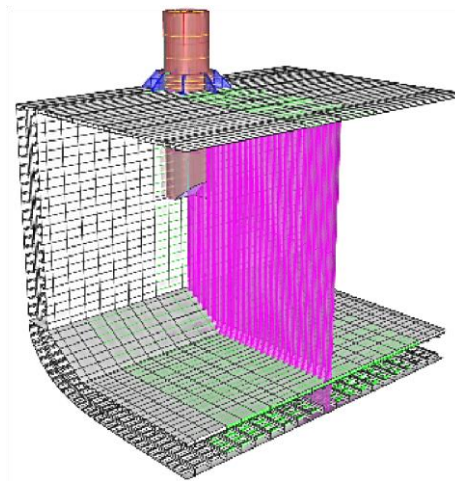


Figure 14. 3D model of the crane pedestal support frame used for the structural analysis of the main deck of the FPSO vessel. This model is done using Rhinoceros software.

Table 5. Properties of the structural steel used for the FEM simulations of the crane pedestal support frame

Property	Value
Density	7850 kg/m ³
Tensile strength	2.5 x 10 ⁸ Pa
Elastic compression limit	2.5 x 10 ⁸ Pa
Maximum tensile strength	4.6 x 10 ⁸ Pa

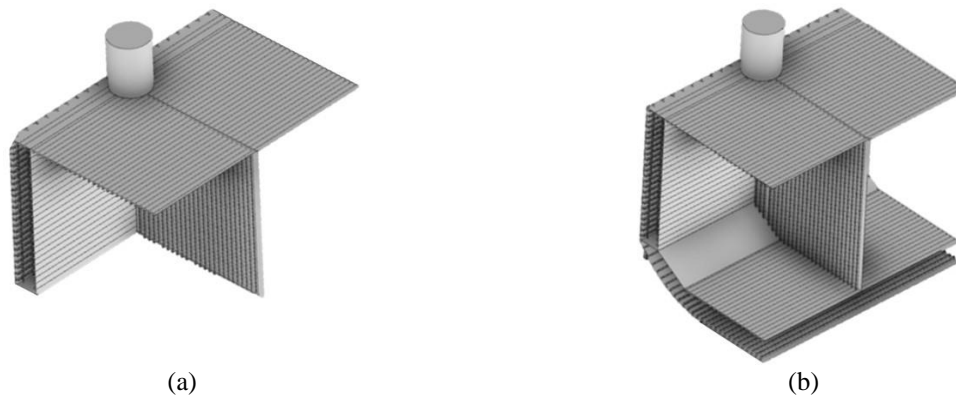


Figure 15. (a) Geometry A of the crane pedestal support frame that regards a part the main deck with the crane pedestal to the waterline; (b) Geometry B that comprises the full 3D model of the crane pedestal support frame.

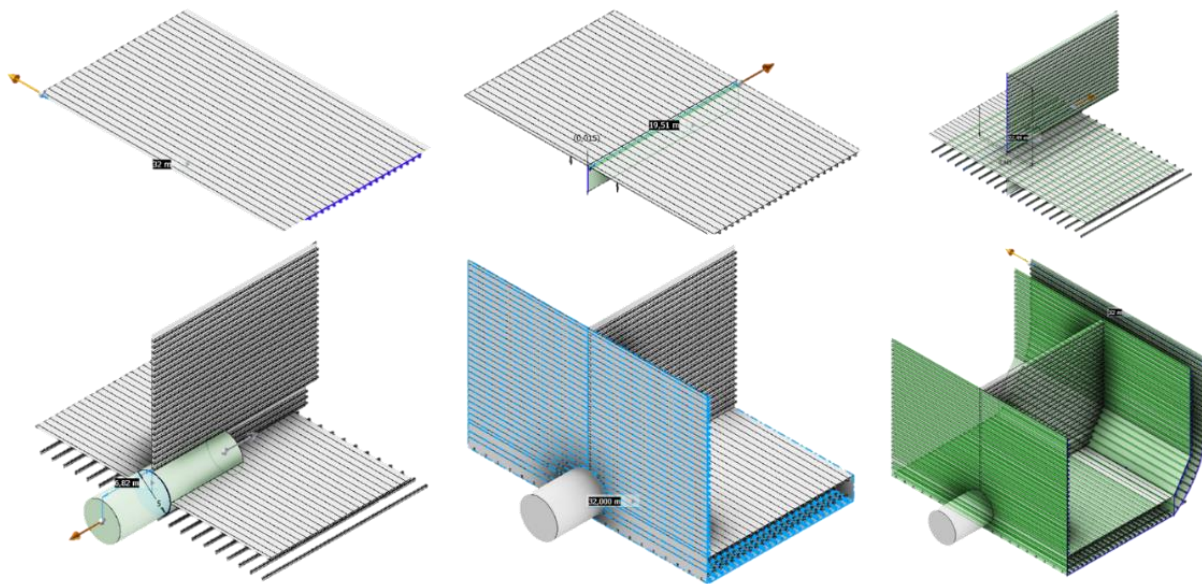


Figure 16. View of the different components of a 3D model of the crane pedestal support frame of the main deck of the FPSO vessel supporting an offshore crane. This 3D model was developed using Inventor software.

Figure 17(a) and (b) depicts the geometrical boundary conditions of the 3D model of the crane pedestal support frame, in where the edges from the geometries A and B are considered fixed. Figure 18 illustrates the maximum force and moment vectors on the crane pedestal.

Furthermore, the Earth's gravity is included in both geometries A and B. The maximum force and moment values are defined using the maximum acceleration on the crane components under the regular operating and hurricane conditions during the navigation of the FPSO vessel.

3. Results and Discussion

3.1. Operational Condition (Calm Sea)

The structural analysis of the offshore crane for its different operating points on both bow and aft sections of the FPSO vessel was studied through FEM models. In each operating point, the maximum von Mises stress of the FEM model of the crane pedestal support frame was determined. Table 6 shows the maximum von Mises stress of the FEM model for each operating point of the crane on the bow section of the vessel using the proposed geometries A and B under regular operating conditions (calm sea).

Figure 19 illustrates the distribution of von Mises stress on the FEM model for the geometry A on the bow section of the vessel. The maximum von Mises stress (134.64 MPa) occurs at the join between the bottom of the crane pedestal and the support frame. Thus, the maximum stresses are reported around this join point. Table 7 depicts the maximum von Mises stress of the FEM model for each operating point of the crane on the aft section of the vessel, employing the proposed geometries A and B under regular operating conditions (calm sea).

Figure 20 depicts the behavior of the von Mises stresses of the FEM model for the geometry B on the aft section of the vessel. The maximum von Mises stress of 119.73 MPa is placed in the connection between the bottom of

the crane pedestal and the support frame. For this case, the stresses register better uniform distribution around of the connection surface of the pedestal and support frame, which allows a safe structural condition for the performance of the offshore crane. For both bow and aft sections, the maximum von Mises stress in the different operating points of the crane for geometry B presents less value than that of geometry A. For this geometry B on both bow and aft sections, the maximum von Mises stress for each operating points registers a value close to 119.73 MPa, which is less than the tensile strength (250 MPa) of the structural steel. It allows a safe structural operation for the offshore crane under regular operating conditions (calm sea).

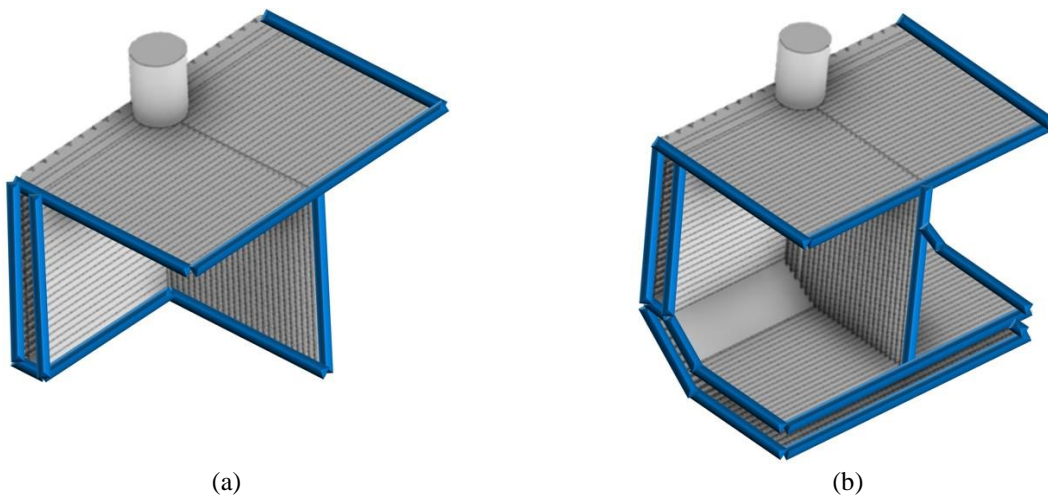


Figure 17. Geometrical boundary conditions (fixed) in the edges of the 3D models of the crane pedestal support frame: (a) geometry A and (b) geometry B.

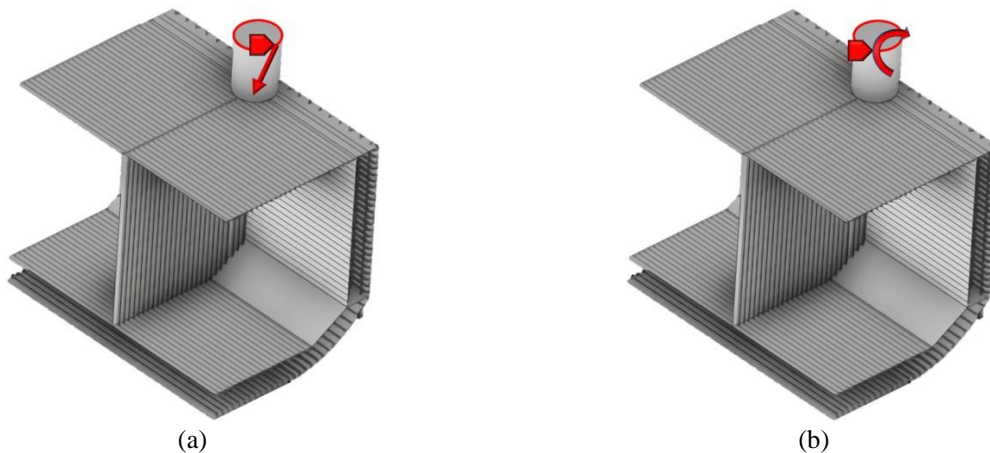


Figure 18. 3D model of the crane pedestal support frame of geometry B, including the maximum (a) force and (b) moment vectors.

3.2. Hurricane Conditions (Storm)

In hurricane condition (storm), the structural analysis of the offshore crane on both bow and aft sections of the FPSO vessel was obtained through FEM models. Considering two operating points (cab and rest), the maximum von Mises stress of the FEM model of the crane pedestal support frame was estimated. Table 8 depicts the maximum von Mises stress of the FEM model for two operating points of the crane on the bow section of the vessel, employing the proposed geometries A and B under hurricane conditions (storm). Table 9 reports the

maximum von Mises stress of the FEM model in two operating points (cab and rest) of crane on the aft section of the vessel regarding the geometries A and B under hurricane condition. For both bow and aft sections, the maximum von Mises stress (cab and rest operating points) of the crane of geometry B registers less magnitude than that of geometry A. For this geometry B on both bow and aft sections, the maximum von Mises stress has a value close to 119.74 MPa, which is less than the tensile strength (250 MPa) of the structural steel. It ensures a safe structural performance for the offshore crane under hurricane conditions (storm).

Table 6. Maximum von Mises stress of the FEM model of the crane pedestal support frame considering five different operating points of the crane on the bow section of the FPSO vessel

Operating point	Nomenclature	Geometry A Maximum von Mises stress (MPa)	Geometry B Maximum von Mises stress (MPa)
1	DP 0	134.67	119.74
2	DP 1	134.64	119.73
3	DP 2	134.64	119.72
4	DP 3	134.64	119.73
5	DP 4	134.65	119.74

*These results regard both geometries A and B under regular operating conditions (calm sea).

Table 7. Maximum von Mises stress of the FEM model of the crane pedestal support frame regarding five different operating points of the crane on the aft section of the FPSO vessel

Operating point	Nomenclature	Geometry A Maximum von Mises stress (MPa)	Geometry B Maximum von Mises stress (MPa)
1	DP 5	134.66	119.74
2	DP 6	134.65	119.73
3	DP 7	134.65	119.73
4	DP 8	134.65	119.74
5	DP 9	134.66	119.75

* These results consider both geometries A and B under regular operating conditions (calm sea).

Table 8. Maximum von Mises stress of the FEM model of the crane pedestal support frame considering two operating points (cab and rest) of the crane on the bow section of the FPSO vessel

Operating point	Nomenclature	Geometry A Maximum von Mises stress (MPa)	Geometry B Maximum von Mises stress (MPa)
Cabin	DP 10	134.67	119.73
Rest	DP 11	134.64	119.73

*These results include both geometries A and B under hurricane conditions (storm).

Table 9. Maximum von Mises stress of the FEM model of the crane pedestal support frame considering two operating points (cab and rest) of the crane on the aft section of the FPSO vessel

Operating point	Nomenclature	Geometry A Maximum von Mises stress (MPa)	Geometry B Maximum von Mises stress (MPa)
Cabin	DP 12	134.67	119.75
Rest	DP 13	134.67	119.75

*These results comprise both geometries A and B under hurricane conditions (storm).

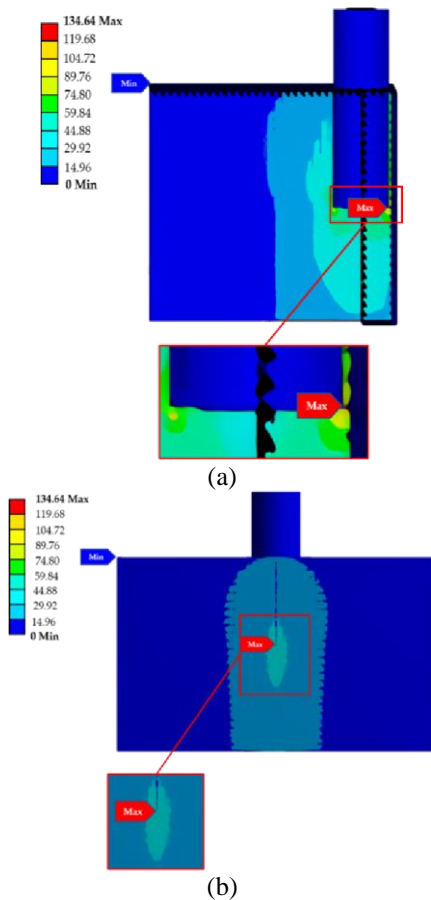


Figure 19. Distribution of von Mises stress of the FEM model of the crane pedestal support frame for the geometry A, considering the crane in bow section of the vessel and under regular operating conditions: (a) profile view and (b) side view.

For both environment conditions, the better results were obtained for the FEM model of the geometry B. This FEM model registers von Mises stresses with less values than those obtained using geometry A. The maximum von Mises stresses of the FEM model for geometry B have approximately a relative difference close to 11.09% in comparison with those of the FEM model for geometry A.

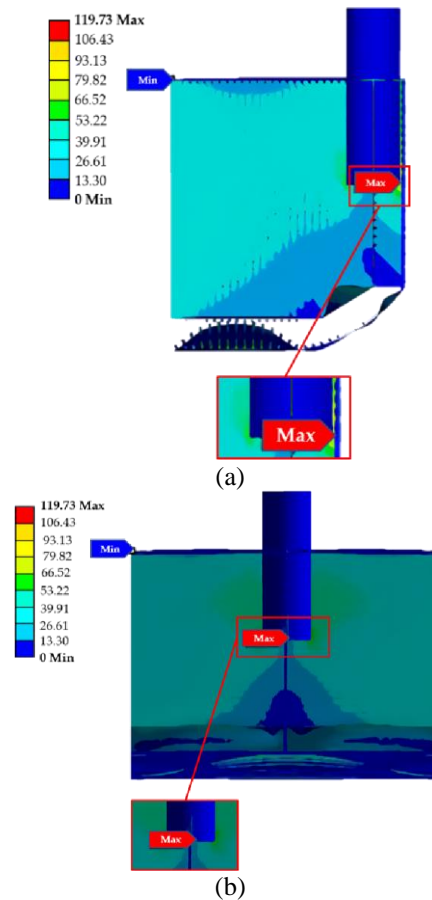


Figure 20. Distribution of von Mises stress of the FEM model of the crane pedestal support frame for the geometry B, including the crane on aft section of the vessel and under regular operating conditions: (a) profile view and (b) side view.

In addition, the geometry B shows better uniform distribution of von Mises stress. This is due to that the FEM model of geometry B includes more structural components, which is closer to real structural members of the main deck supporting the offshore crane.

3.3. Permissible Stress

According to DNV-GL classification society [16], the maximum permissible stress (σ_p) of the longitudinal hull girder structural members can be established by:

$$\sigma_p = \sigma_Y \eta \quad (16)$$

where η is the permissible yield utilization factor (0.80 for longitudinal hull girder structural members, supporting structural components and bulkheads) of the FEM model and σ_Y is the tensile strength of the material (250 MPa for structural steel).

Based on this criterion of DNV-GL classification society and considering the different operating points of the crane on the bow and aft sections of the vessel, the maximum von Mises stresses of the FEM model for both geometry A and B are less than the permissible stress (200 MPa) under the calm sea and storm environment conditions (Table 10). Thus, the main deck of the FPSO vessel and offshore crane can have a safe structural behavior for the different loads and environment conditions studied in this work.

4. Conclusions

A methodology to estimate the structural behavior of a main deck of FPSO vessel supporting a BOS 2600 offshore crane was reported. This methodology included the hydrodynamic conditions on the FPSO vessel using environmental data from Gulf of Mexico with a return period of 10 and 100 years. This structural behavior was studied under two different operating conditions (calm sea and storm) using FEM models and rules of DNV-GL

classification society. In addition, this methodology regarded critical operating points of the crane on both bow and aft sections of the FPSO vessel. The results of the structural analysis showed uniform distribution of the von Mises stress of the crane pedestal support frame. The von Mises stress showed uniform distribution in the structure of the vessel section with a maximum stress concentration at the crane pedestal base. The structural reinforcements of the main deck, bulkheads, double bottom and bottom helped to decrease the maximum stresses. The maximum values of von Mises stress were less than the maximum permissible stress of the structural steel of the main deck and crane pedestal, which allowed a safe structural performance.

Dynamic amplification factors are generally used in naval engineering conventional structural analyses to establish safe parameters and obtain conservative results. However, these conservative results can increase the costs of the naval structures. The proposed methodology can be used to predict safe installation points for operation of offshore cranes on main deck of FPSO vessels under different operating and environmental conditions. Thus, our methodology can estimate the structural behavior of FPSO vessels in specific operating areas, which contributes into better results that decrease the use of materials and man-hours in construction work, repair or modification. This process represents a significant economic saving in long term and optimal data in analyses required for FPSO vessel certification.

Acknowledgment

The authors acknowledge the support of the Universidad Veracruzana.

Table 10. Comparison of the results of maximum von Mises stress of the FEM model of the crane pedestal support frame with respect to the maximum permissible stress indicated by the DNV-GL classification society

Case	Maximum von Mises stress (MPa)		Maximum permissible stress (MPa)		Status	
	Geometry A	Geometry B	Geometry A	Geometry B	Geometry A	Geometry B
Bow section, operative condition	134.67	119.74	200	200	Safe	Safe
Aft section, operative condition	134.66	119.75	200	200	Safe	Safe
Bow section, hurricane condition	134.67	119.73	200	200	Safe	Safe
Aft section, hurricane condition	134.67	119.75	200	200	Safe	Safe

Sources: [16].

Funding

This research received no external funding.

Autor Contributions

D. Hernández-Ménez: Conceptualization, Methodology, Formal analysis, Investigation, Writing - Original Draft.
I. Félix-González: Formal analysis, Investigation, Writing - Original Draft.
J. Hernández-Hernández: Formal analysis, Investigation, Writing - Original Draft.
A. L. Herrera-May: Conceptualization, Formal analysis, Investigation, Writing - Review & Editing.

All authors have read and agreed to the published version of the manuscript.

Conflicts of Interest

The authors declare no conflict of interest.

Institutional Review Board Statement

Not applicable.

Informed Consent Statement

Not applicable.

Reference

- [1] J. S. Templeton, "Jack-up Spud Can Foundation Fixity for Various Clay Strength Profiles," in *SNAME 24th Offshore Symposium*, 2019.
- [2] P. A. Gale, *Design, The Ship Design Process. In Ship Design and Construction*, Society of Naval Architects and Marine Engineers: Jersey City, USA, 2003.
- [3] U. Sood, "Assessment of Lifting Criteria for Crane on a Heavy Lift Ship Load Check and Fatigue Life Calculation", Master Thesis, University of Rostock, 2017.
- [4] American Petroleum Institute, *Recommended Practice for Planning, Designing and Constructing Fixed Offshore Platforms — Working Stress Design, 21th ed.* API: Australia, 2000.
- [5] O. Ozguc, "The assessment of impact damage caused by dropped objects on floating offshore structures," *Proc. IMechE Part M: J. Engineering for the Maritime Environment*, vol. 235, no. 2, pp. 491-510, 2021, doi: <https://doi.org/10.1177/1475090220972586>
- [6] S. Lee, S. Lee, S. Kwon, "Effects of Topside Structures and Wind Profile on Wind Tunnel Testing of FPSO Vessel Models," *J. Mar. Sci. Eng.*, vol. 8, no. 6, 2020, <https://doi.org/10.3390/jmse8060422>
- [7] J. Shin, "Load-spectrum models for offshore crane fatigue analysis," *International Journal of Offshore and Polar Engineering*, vol. 31, no. 4, pp. 480-486, <https://doi.org/10.17736/ijope.2021.hc22>
- [8] B. N. Khudhur, "Finite element analysis of the boom of crane loaded statically," *Eng. Technol. J.*, vol. 31, pp. 1626-1639, 2013, doi: <https://doi.org/10.30684/etj.2013.82179>
- [9] J. Krukowski, A. Maczyński, "Application of the rigid finite element method for modelling an offshore pedestal crane," *Arch. Mech. Eng.*, vol. 60, pp. 451-471, 2013, doi: <https://doi.org/10.2478/meceng-2013-0028>
- [10] T. Tuswan, K. Abdullah, A. Zubaydi, "Budipriyanto, A., Finite-element analysis for structural strength assessment of marine sandwich material on ship side-shell structure," *Mater. Today: Proc.*, vol. 13, pp. 109-114, 2019, doi: <https://doi.org/10.1016/j.matpr.2019.03.197>
- [11] C.M. Salazar-Domínguez, J. Hernández-Hernández, E. D. Rosas-Huerta, G. E. Iturbe-Rosas, A.L. Herrera-May, "Structural Analysis of a Barge Midship Section Considering the Still Water and Wave Load Effects," *J. Mar. Sci. Eng.*, vol. 9, 2021, doi: <https://doi.org/10.3390/jmse9010099>
- [12] DNV-GL, 2022. [Online]. Available: <https://rules.dnv.com/docs/pdf/DNV/ST/201909/DNVGL-ST-0378.pdf>
- [13] DNV-GL, 2022. [Online]. Available: <https://www.dnv.com/rules-standards>
- [14] LIEBHERR, 2022. [Online]. Available: <https://www.liebherr.com/es/col/productos/gruas-maritimas/gruas-maritimas.html>
- [15] D.F. Hernández-Ménez, "Structural Analysis of Main Deck of a FPSO Vessel Supporting an Offshore Crane (Translation of Spanish)," Master Thesis, Universidad Veracruzana, Mexico, 2020.
- [16] DNV-GL, 2022. [Online]. Available: <https://rules.dnv.com/docs/pdf/DNV/RU-SHIP/2018-07/DNVGL-RU-SHIP-Pt3Ch7.pdf>